AMERICAN JOURNAL OF PHYSICAL ANTHROPOLOGY 104:117–131 (1997)

Cortical Bone Distribution in the Femoral Neck of Hominoids: Implications for the Locomotion of *Australopithecus afarensis*

JAMES C. OHMAN,[1]* TODD J. KROCHTA,[2] C. OWEN LOVEJOY,[3,4,5] ROBERT P. MENSFORTH,[6] AND BRUCE LATIMER[3,4,7]
[1]*Hominid Palaeontology Research Group, Department of Human Anatomy and Cell Biology, New Medical School, University of Liverpool, Liverpool L69 3GE, United Kingdom*
[2]*LumenX Company, Division of Alltrista, Mogadore, Ohio 44260*
[3]*Department of Anthropology and Biological Anthropology Program, Division of Biomedical Sciences, Kent State University, Kent, Ohio 44242*
[4]*Laboratory of Physical Anthropology, Cleveland Museum of Natural History, Cleveland, Ohio 44106*
[5]*Department of Orthopaedic Surgery, School of Medicine, Case Western Reserve University, Cleveland, Ohio 44106*
[6]*Department of Anthropology, Cleveland State University, Cleveland, Ohio 44115*
[7]*Department of Anatomy, Case Western Reserve University, Cleveland, Ohio 44106*

KEY WORDS hominid locomotion; functional morphology; computed tomography

ABSTRACT Contiguous high resolution computed tomography images were obtained at a 1.5 mm slice thickness perpendicular to the neck axis from the base of the femoral head to the trochanteric line in a sample of 10 specimens each of *Homo sapiens*, *Pan troglodytes*, and *Gorilla gorilla*, plus five specimens of *Pan paniscus*. Superior, inferior, anterior, and posterior cortical thicknesses were automatically measured directly from these digital images. Throughout the femoral neck *H. sapiens* displays thin superior cortical bone and inferior cortical bone that thickens distally. In marked contrast, cortical bone in the femoral neck of African apes is more uniformly thick in all directions, with even greater thickening of the superior cortical bone distally. Because the femoral neck acts as a cantilevered beam, its anchorage at the neck-shaft junction is subjected to the highest bending stresses and is the most biomechanically relevant region to inspect for response to strain. As evinced by A.L. 128-1, A.L. 211-1 and MAK-VP-1/1, *Australopithecus afarensis* is indistinguishable from *H. sapiens*, but markedly different from African apes in cortical bone distribution at the femoral neck-shaft junction. Cortical distribution in the African ape indicates much greater variation in loading conditions consistent with their more varied locomotor repertoire. Cortical distribution in hominids is a response to the more stereotypic loading pattern imposed by habitual bipedality, and thin superior cortex in *A. afarensis* confirms the absence of a significant arboreal component in its locomotor repertoire. Am J Phys Anthropol 104:117–131, 1997.

In a review of the evolution of hominid bipedality, Lovejoy (1988) described the pattern of morphological adaptations manifested in the pelvis and proximal femur.

*Correspondence to: James C. Ohman, Hominid Palaeontology Research Group, Department of Human Anatomy and Cell Biology, New Medical School, University of Liverpool, Liverpool L69 3GE, United Kingdom. E-mail: J.C.Ohman@liverpool.ac.uk

Received 14 August 1995; accepted 7 July 1997.

Among the features presented was a marked difference between bipedal hominids and quadrupedal apes in the distribution of cortical bone in the femoral neck at the neck-shaft junction. In the chimpanzee, a cross section of the femoral neck "reveals a central marrow-filled channel surrounded by a thick layer of dense bone" (Lovejoy, 1988, p. 88). This contrasts with the cross section of a hominid femoral neck wherein "the outer ring of solid bone is thick only at the bottom, and the rest of the neck is bounded by a thin shell of bone" (Lovejoy, 1988, p. 88). As with the other evidence, Lovejoy (1988) provided the functional significance of these two distinct cortical distribution patterns; that is, the pattern of habitual bipedality in hominids vs. that of quadrupedality in apes (see below).

Subsequently, however, Stern and Susman (1991) questioned the evidence presented by Lovejoy (1988). Specifically, they (Stern and Susman, 1991) stated:

> Thin cortical bone along the superior aspect of the femoral neck in conjunction with thick cortical bone along its inferior aspect has been said to indicate human-like bipedalism and to be incompatible with arboreal behavior. We challenge the notion that such cortical bone distribution constitutes a magic trait. We have found a greater similarity between cortical bone distribution in the femoral necks of some nonhuman primates than was previously documented [p. 100].

The present study reports femoral neck cortical distribution and its biomechanical implications in a sample of *Homo sapiens*, *Pan paniscus*, *Pan troglodytes*, *Gorilla gorilla*, and three specimens of *Australopithecus afarensis*. We also evaluate bone distribution in the femoral neck with respect to Stern and Susman's (1991) concept of a "magic trait."[1]

SKELETAL MATERIAL

The extant hominoid sample included one femur from 10 specimens each of *H. sapiens*, *P. troglodytes*, *G. gorilla*, and five specimens of *P. paniscus* (Table 1). All specimens were nonpathological. The African apes were all wild-shot adults, as defined by epiphyseal synostosis. To control for age-related osteopenia in *H. sapiens*, accompanying records were used to limit the sample to individuals whose ages-at-death were between 20 and 29 years. Adult African apes exhibit little or no age-related osteopenia (Ohman et al., 1997; *contra* Sumner et al., 1989), so there was no need to control for the age-at-death of individuals in these taxa (see also below).

TABLE 1. Skeletal material

Species	Sex		Source
	Male	Female	
Homo sapiens	5	5	Cleveland Museum of Natural History
Gorilla gorilla	5	5	Cleveland Museum of Natural History
Pan troglodytes	5	5	Cleveland Museum of Natural History
		1[a]	American Museum of Natural History
Pan paniscus	2	1	Museum of Comparative Zoology
		1	Museum Royale l'Afrique Centrale

[a] Contralateral leg is pathological; field notes state that this was a pregnant female.

DATA ACQUISITION

For each femur, contiguous computed tomography (CT) images were obtained at a 1.5 mm slice thickness perpendicular to the neck axis from the base of the femoral head to the trochanteric line. All CT images were saved for direct digital analyses. Hard copy films were also obtained.

The femora of *H. sapiens*, *P. troglodytes*, and *G. gorilla* were scanned in air with a Picker International PQ 2000 CT Scanner in the half field at 130 kV and 65 mA for 2 sec. The images were reconstructed in a 512^2 matrix and a 10 cm field of view using an ultrahigh resolution algorithm, so the size of each pixel was known to be approximately 0.1953 mm along a side. These scan parameters and the reconstruction algorithm were chosen to obtain the best possible spatial resolution, which on the Picker International PQ 2000 is 20 lp/cm or 0.25 mm.[2]

The scarcity of *P. pansicus* femora made the acquisition of their CT images more

[1] As defined by Stern and Susman (1991) a "magic trait" is "a single anatomical/biomechanical trait that will tell us everything we wish to know about the locomotion of an early hominid . . . [and] when it is found it will not only reveal how the animal performed its customary activities, it will also notify us of behaviors that were no longer adaptively significant" (p. 100).

[2] "The spatial resolution of a CT unit is its ability to portray small structures that are separated only slightly in the object" (Hendee, 1983, p. 71).

difficult. The single specimen housed at the American Museum of Natural History was CT scanned in the Department of Radiology, New York University Medical Center. The three specimens housed at the Museum of Comparative Zoology were CT scanned in the Department of Radiology, Dana Farber Cancer Institute. The single specimen obtained from the Musee Royale de l'Afrique Centrale was scanned in the Department of Radiology, University of Colorado Health Sciences Center.[3]

Despite being obtained at three different institutions, all specimens of *P. pansicus* were scanned on General Electric (GE) 9800 HiLight CT Scanners with identical parameters. These were chosen to obtain the best possible spatial resolution, and thus closely match the image quality obtained for the other taxa. Each femur was scanned in air in the small scan field at 120 kV and 70 mA for 2 sec. The images were reconstructed in a 512^2 matrix and a 9.6 cm field of view using GE's edge algorithm, so the size of each pixel was known to be approximately 0.1875 mm along a side. The obtained spatial resolution was 0.35 mm (Bruce Teeter, personal communication).

CT IMAGE ANALYSIS

A CT image is actually a digital matrix of pixels, or picture elements. In turn, each pixel represents a voxel, or volume element, whose third dimension is the thickness of the slice. The value of each pixel represents the voxel's attenuation, and is expressed in Hounsfield Units (HUs), which increase with increasing attenuation and are normalized such that water and air have values of zero and −1,000, respectively. For typical x-ray energies used in CT, attenuation is largely the result of tissue density (e.g., Christensen et al., 1978). Therefore, bone is characterized by large HUs in CT images.

Given a CT cross sectional image of a small solid cylindrical homogeneous object scanned in air, a profile can be plotted of HUs vs. pixels across a row through the center of the object (Fig. 1A). As one moves across the profile in Figure 1A and the edge of the object is reached, the profile increases distinctly through a steep gradient to the HU for the object, levels off and then decreases rapidly as the other edge of the object is reached. The two gradients representing the two edges of the object are not truly vertical, but instead have a steep slope with the two true edges of the object occurring somewhere within these two gradients. The steepness of the slope is dependent upon the differential attenuation across the boundary, the reconstruction algorithm used, and the spatial resolution of the CT scanner. In this study we used these criteria to maximize boundary slopes: 1) bone with high attenuation was scanned in air which has essentially no attenuation; 2) an ultrahigh resolution reconstruction algorithm was used; and 3) modern high resolution CT scanners were used.

It is an accepted practice that the true width of the object occurs at half the maximum HU, or "full width at half maximum" (FWHM) (e.g., Koehler et al., 1979; Sprawls, 1987; Zatz, 1981). Similarly (Fig. 1B), cortical bone is relatively dense and homogeneous, and in a CT image an a priori assumption can be made that a steep gradient in HUs exists at the bone's boundaries. Therefore, FWHM can be applied in order to locate true bone boundaries with great accuracy.

This approach (i.e., FWHM) has been used to accurately locate boundaries for linear measurements of bone and dental enamel (e.g., Ohman, 1993b; Ohman and Krochta, in press; Spoor et al., 1993, 1994). Indeed, Spoor et al. (1993) recently reported an empirically determined "maximum error range of ±0.1 mm" (p. 469) for linear measurements of cortical bone and dental enamel in CT images obtained with a spatial resolution of 0.5 mm. Thus, using FWHM to locate high contrast bone boundaries Spoor et al. (1993) produced results whose accuracy was actually better than the obtained spatial resolution.

Another theoretical approach to estimate accuracy for FWHM yields a similar conclusion. Given the extremely steep periosteal and endosteal gradients present in CT images of bone scanned in air with parameters like those used here, the potential error introduced by the FWHM threshold is at most ±1 pixel for each gradient, or ±2 pixels

[3]This specimen was on loan to Dr. David Begun.

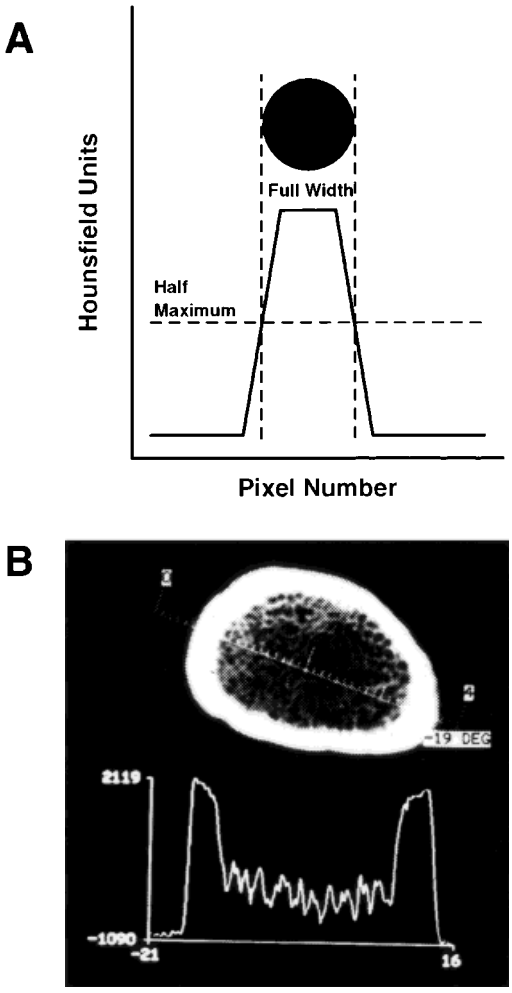

Fig. 1. **(A)** Full width at half maximum. **(B)** Typical superoinferior profile of Hounsfield units across a femoral neck.

for each cortical thickness or neck diameter. In this study each pixel was known to be at most 0.1953 mm along a side, so potential error due to FWHM around each cortical thickness or neck diameter should be at most ±0.3906 mm. Therefore, the potential error due to FWHM is again likely to be less than that introduced by the inherent spatial resolutions of the CT scanners used, which were at most ±0.35 mm for each bone boundary, or at most ±0.70 mm for each cortical thickness or neck diameter. Thus, the obtained spatial resolution around each boundary remains a conservative general estimate of plus or minus error for CT images.

Superoinferior and anteroposterior diameters, as well as superior, inferior, anterior and posterior cortical thicknesses were automatically computed across superoinferior and anteroposterior profiles through the femoral neck for each digital CT image. The orientation of the profiles was maintained for each specimen. Given the known pixel size, diameters and thickness measurements were thus obtained via image analysis at a threshold equal to the FWHM value for each profile.

For *H. sapiens*, *P. troglodytes* and *G. gorilla*, image analyses were performed in the PIPP (Picker Image Processing Package) environment using the computer language C on the Tower configuration of Picker International's SUPS (Single User Pyramid System) computer. For *P. paniscus*, images were loaded on a Silicon Graphics Indy SC Workstation, and profiles were obtained and written to ASCII files using ANALYZE (Biomedical Imaging Resource, Mayo Foundation). Metrics were then automatically computed from these profiles on a MS-DOS (Microsoft Corporation) based personal computer using software written in Turbo Basic (Borland International, Inc.).

For each specimen, superior and inferior cortical areas were measured from the CT image obtained at the neck-shaft junction. A superoinferior axis was defined as a line connecting the most superior and most inferior points, and the superior and inferior halves were established by an orthogonal line through the midpoint of the superoinferior axis. Superior and inferior cortical areas were then measured from hard copy of the analog CT images using a Summagraphics 2-D digitizer tablet.

Thus, unlike diameters and cortical thicknesses, an image analysis approach was not used to measure cortical areas. Linear distance measurements are easily computed along a line of pixels defined by the user (see above), whereas areal measurements require the accurate identification of *both:* 1) every pixel that does belong to the object of interest; and 2) every pixel that does *not* belong to the object of interest. When cancellous bone is absent or minimal in a CT image (e.g., at midshaft), accurate identification of only cortical bone is relatively straightfor-

ward (Ohman, 1993a, in review; Ohman and Krochta, in press). However, when the cortical shell is filled with cancellous bone (e.g., in the femoral neck), it is difficult to differentiate pixels representing cortical bone from those representing trabeculae. Any single trabecula has a similar density, and therefore a similar HU, as that of cortical bone.[4] Thus, with image analysis techniques (e.g., threshholding, autocontouring, or region growing) it is very easy to identify every pixel that represents cortical bone, but at the same time it is very difficult to eliminate those pixels that represent trabeculae. Therefore, we chose to manually measure cortical area, and, for simplicity, did so from hard copy of the analog CT images. This approach probably produced cortical area data that are less accurate than those data obtained for diameters and cortical thicknesses. Nonetheless, the cortical area results are consistent with the cortical thickness results (see below), as well as with cortical areas measured from physical sections (see Lovejoy et al., in review).

RESULTS

Figures 2 and 3 show relative anterior and posterior cortical thicknesses along the length of the neck in *H. sapiens* and the African apes. For ease of comparison, neck lengths have been standardized such that the base of the head is 0% and the neck-shaft junction is 100% (horizontal axis). Similarly, for each section the cortical thicknesses have been standardized as a percentage of the neck diameter measured in that section (vertical axis). Although relative cortical thicknesses are slightly thinner in *H. sapiens*, all taxa display generally uniform anterior and posterior cortical thicknesses along the neck. In addition, in all taxa the cortices tend to thicken slightly from the head to the neck-shaft junction.

Figures 4 and 5 show similar plots for relative superior and inferior cortical thicknesses along the length of the neck. In *H. sapiens* superior cortical thickness remains uniformly thin, while inferior cortical thickness increases in proximity to the neck-shaft junction. The African apes contrast sharply. Their superior cortex is thicker than *H. sapiens* at the base of the head and continues to thicken distally. Inferior cortical thickness in the African apes is both thick and uniform along the neck.

Another way to display these data is by means of a simple ratio between the superior and inferior cortical thicknesses (Fig. 6). In *H. sapiens*, this ratio is consistently low, and *decreases* as the neck-shaft junction is approached. The superior cortical thickness of *H. sapiens* is about one-quarter of inferior cortical thickness at the neck-shaft junction. Again the African apes differ dramatically. Their ratios are more variable, and *increase* distinctly from the head to the neck-shaft junction. Their superior cortical thickness is generally equivalent to or greater than their inferior cortical thickness at the neck-shaft junction.

Because the femoral neck can be modeled as a cantilevered beam (Lovejoy et al., in review), the most biomechanically relevant section occurs at the neck-shaft junction. Figure 7 focuses on this comparison. There is little difference between the species in relative anterior and posterior cortical thickness at this location. However, for both superior over inferior cortical thicknesses and cortical areas, *H. sapiens* is much lower, less variable and does not even approach the African apes in its range. For *H. sapiens* superior cortical thickness is about one-quarter of inferior cortical thickness, and inferior cortical area is about three times greater than superior cortical area. In contrast, in the African apes superior cortical thickness and area are approximately equal to both inferior cortical thickness and area.

FOSSIL EVIDENCE

There are a number of proximal femora of *A. afarensis* that could potentially contribute evidence of femoral neck cortical distribution in this early hominid species (Clark et al., 1984; Johanson et al., 1982a, 1982b; Lovejoy et al., 1982; White, 1984). One of these, the Pliocene MAK-VP-1/1, is from Maka, Ethiopia (Clark et al., 1984; White,

[4]In a CT image the mean HU measured for a region of interest (ROI) in cancellous bone is lower than one comparably obtained in cortical bone because of the greater porosity of cancellous bone. A single trabecula in a CT image may also have a lower HU than typically obtained for cortical bone, but this is due to partial voluming; that is, when a trabecula doe *not* completely fill a voxel, the voxel itself has a lower HU due to its porosity.

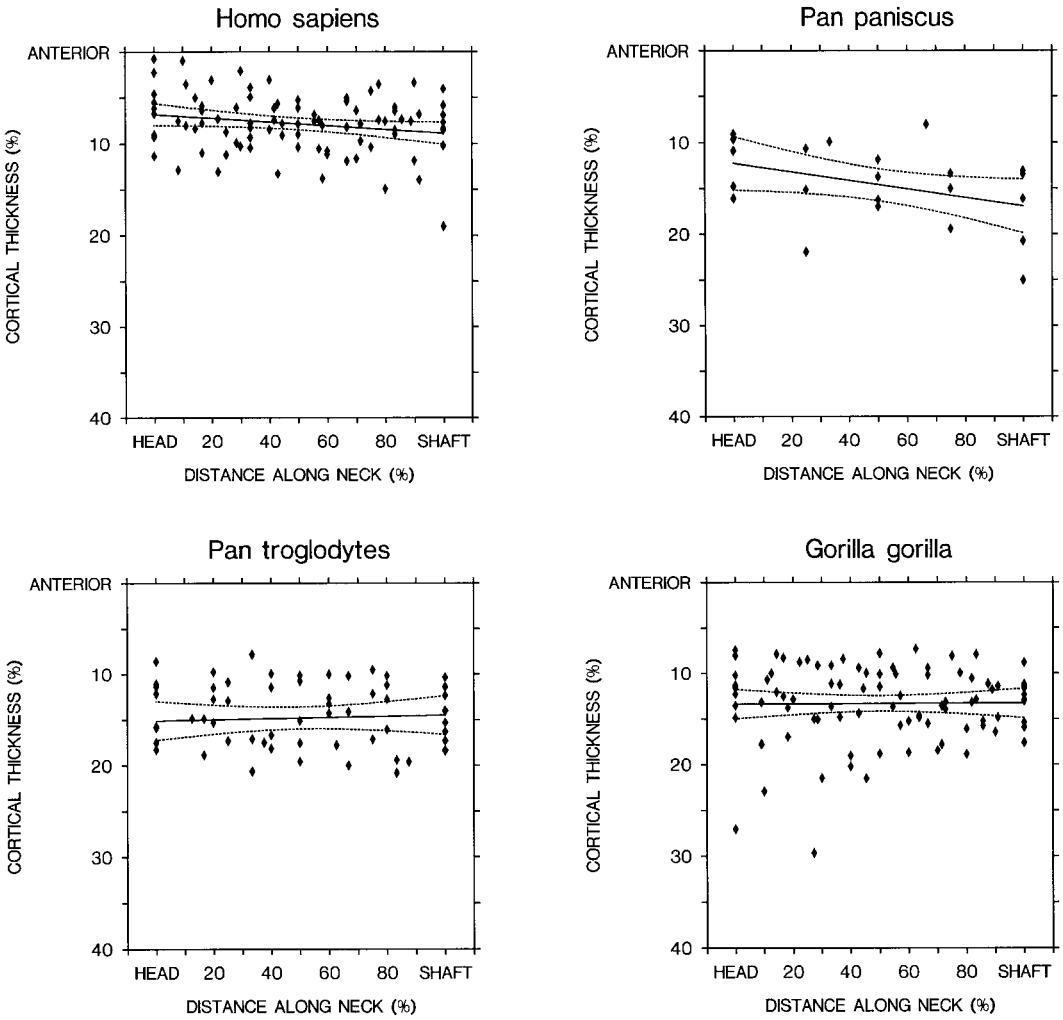

Fig. 2. Relative anterior cortical thicknesses along the femoral neck in *Homo sapiens, Pan paniscus, Pan troglodytes,* and *Gorilla gorilla.* Least squares regression lines with 95% confidence intervals are provided *only to illustrate* typical relative cortical thicknesses along the femoral neck for each taxon, as we do not expect cortical thicknesses to vary linearly (sensu stricto) along the femoral neck.

1984), and its preservation permitted exquisite detail of its radiographic anatomy to be obtained via both radiography and CT. The specimen MAK-VP-1/1 thus provides evidence of its internal morphology with direct bearing on this study. A complete discussion of MAK-VP-1/1 is presented by Lovejoy et al. (in review). The remaining specimens are from the Pliocene Hadar Formation, Ethiopia (Johanson et al., 1982a, 1982b; Lovejoy et al., 1982), and are included in the hypodigm of *A. afarensis* (Johanson et al., 1978). Unfortunately, due to conditions of fossilization, the Hadar specimens are radioopaque, so the internal morphology of most Hadar specimens cannot be evaluated. However, two proximal femora, A.L. 128-1 and A.L. 211-1, were naturally severed at approximately the neck-shaft junction, such that a section of the femoral neck is exposed (Fig. 8). They thus provide direct evidence of their cortical distribution.

Qualitatively A.L. 128-1 and A.L. 211-1 (Fig. 8) clearly demonstrate a remarkable

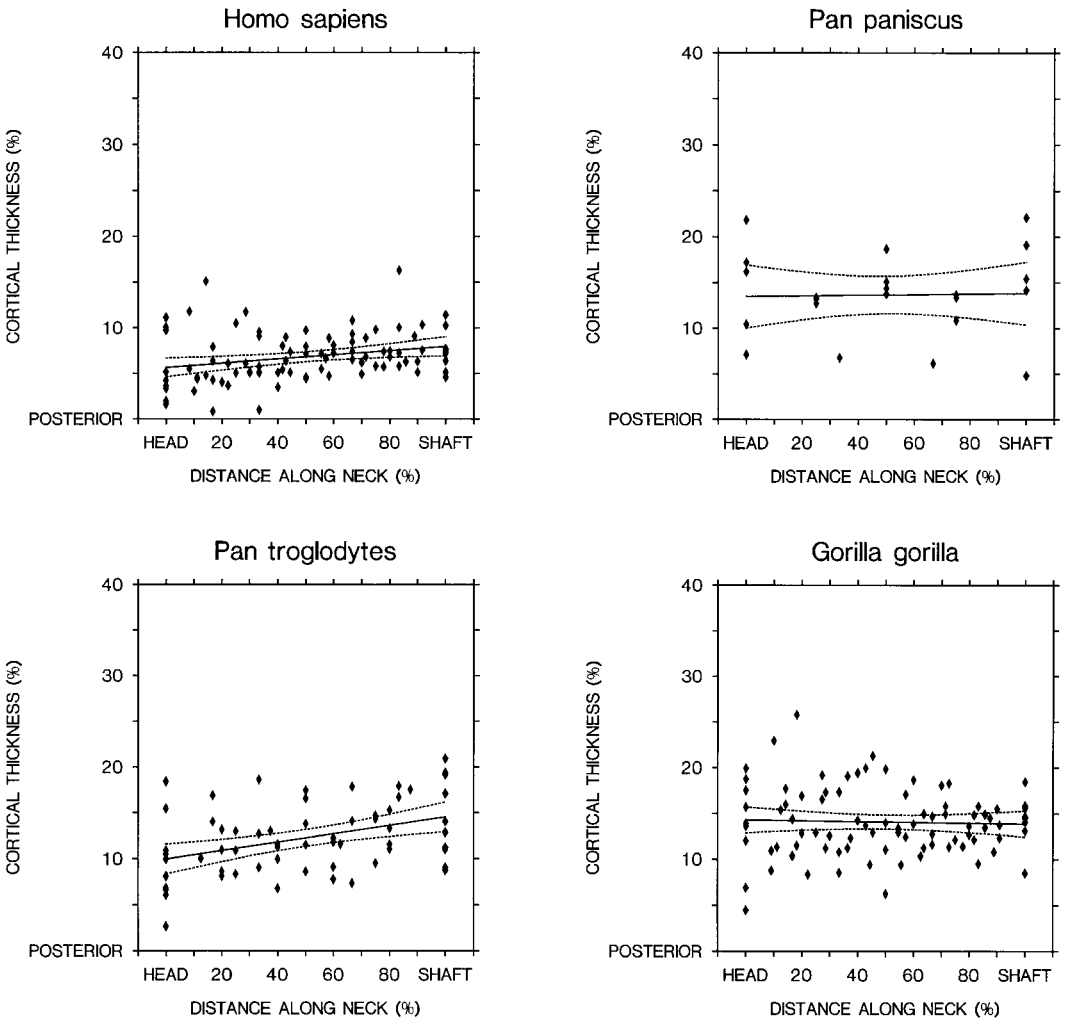

Fig. 3. Relative posterior cortical thicknesses along the femoral neck in *Homo sapiens, Pan paniscus, Pan troglodytes,* and *Gorilla gorilla.* Least squares regression lines with 95% confidence intervals are provided *only to illustrate* typical relative cortical thicknesses along the femoral neck for each taxon, as we do not expect cortical thicknesses to vary linearly (sensu stricto) along the femoral neck.

similarity to *H. sapiens* in cortical distribution. To quantify these observations, cortical thicknesses and neck diameters were directly measured from A.L. 128-1, housed in the National Museum of Ethiopia. Using the method outlined above, superior and inferior cortical areas were also measured from a scaled photograph of A.L. 128-1, housed in the Department of Physical Anthropology at the Cleveland Museum of Natural History. Unfortunately, the superior surface of A.L. 211-1 suffered postmortem damage. While the hominid pattern is clearly present in A.L. 211-1 (Fig. 8), the specimen nevertheless lacks a sufficient portion of its superior neck for measurement. In the ratios of anterior to posterior and superior to inferior cortical thickness, and the ratio of superior to inferior cortical areas (Fig. 6), A.L. 128-1 differs markedly from the African apes and is indistinguishable from *H. sapiens.*

In the description and analysis of a proximal femur of *A. africanus,* MLD 46, from Makapansgat, South Africa, radiographic

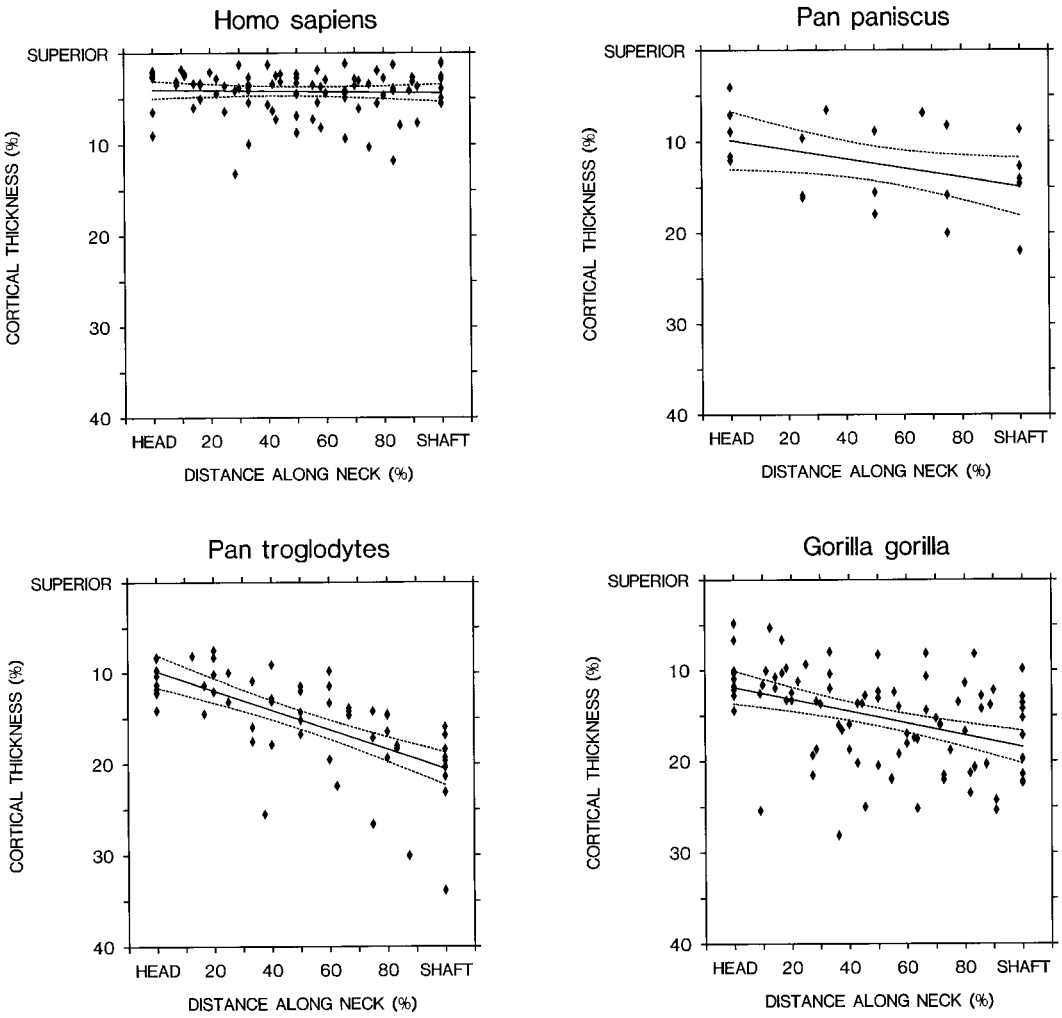

Fig. 4. Relative superior cortical thicknesses along the femoral neck in *Homo sapiens*, *Pan paniscus*, *Pan troglodytes*, and *Gorilla gorilla*. Least squares regression lines with 95% confidence intervals are provided *only to illustrate* typical relative cortical thicknesses along the femoral neck for each taxon, as we do not expect cortical thicknesses to vary linearly (sensu stricto) along the femoral neck.

images "revealed the cortical bone along the inferior margin of the neck to be relatively thicker than that along the superior margin" (Reed et al., 1993, p. 5). We would also expect this pattern to be evident in other specimens (e.g., Stw 101) of this taxon.

DISCUSSION

Throughout the femoral neck, and particularly at the neck-shaft junction, *H. sapiens* is consistently characterized by thin superior cortical bone while its inferior cortical bone progressively thickens distally (see also Walker and Lovejoy, 1985; Lovejoy et al., in review). In contrast, cortical bone in African ape femoral necks is generally more uniformly thick in all directions, with a trend toward further thickening of the superior cortical bone as the neck-shaft junction is approached. Indeed, even in the unlikely event that these African ape proximal femora did display age-related osteopenia (Ohman et al., 1997), our results would be more conservative because they would demonstrate that the femoral necks of *old* African apes (i.e., those with the least amount of

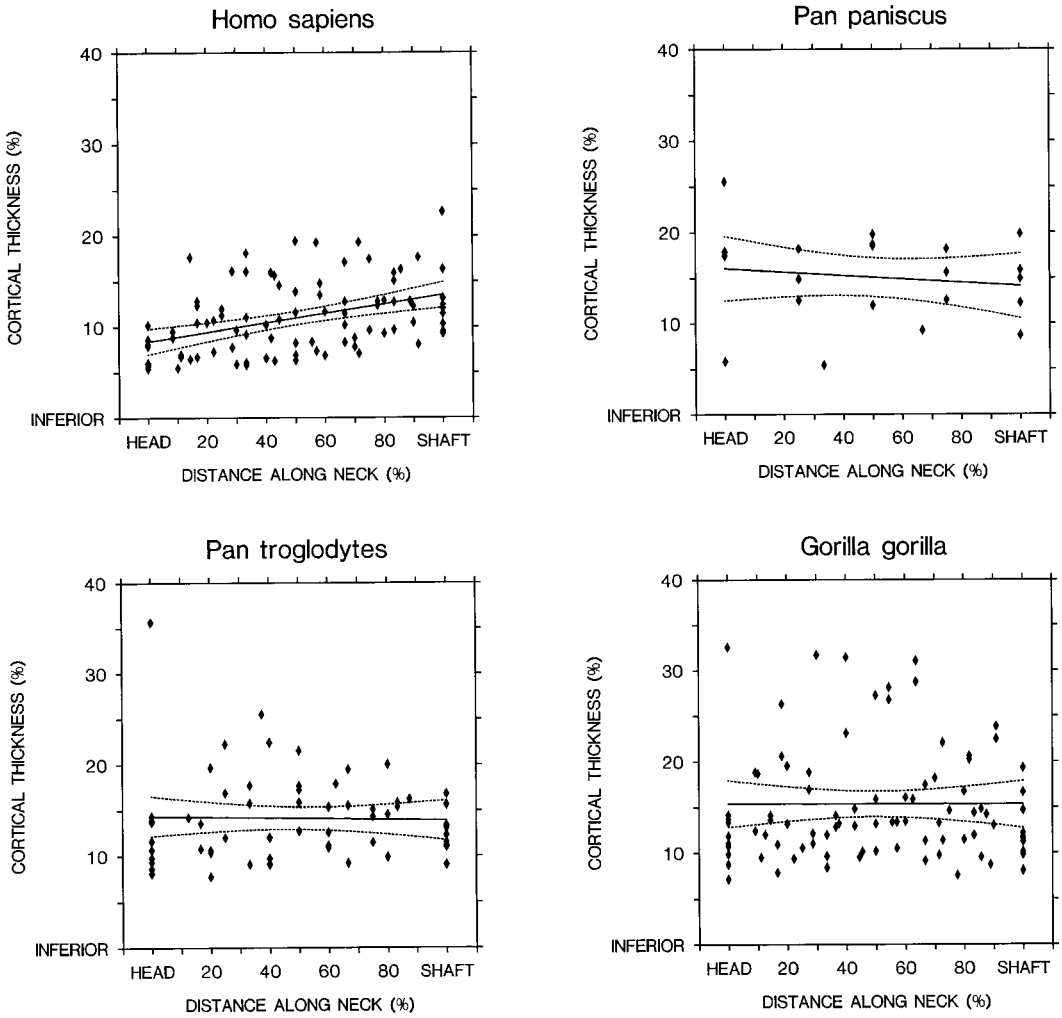

Fig. 5. Relative inferior cortical thicknesses along the femoral neck in *Homo sapiens, Pan paniscus, Pan troglodytes,* and *Gorilla gorilla.* Least squares regression lines with 95% confidence intervals are provided *only to illustrate* typical relative cortical thicknesses along the femoral neck for each taxon, as we do not expect cortical thicknesses to vary linearly (sensu stricto) along the femoral neck.

bone) still have more cortical bone than the femoral necks of *young* adult humans (i.e., those with the greatest amount of bone).

These results thus directly contradict claims made by Stern and Susman (1991). While they (Stern and Susman, 1991) did find that their single gorilla specimen possessed thicker superior than inferior cortical bone, they at the same time asserted that in their "other nonhuman specimens (one each of spider monkey, siamang, common chimpanzee, and pygmy chimpanzee) the inferior cortical bone was thicker" (pp. 103–105).

Unfortunately, a direct comparison between our results and theirs (Stern and Susman, 1991) is not possible. First, they (Stern and Susman, 1991) presented only limited qualitative data: one AP radiograph for the spider monkey; and for the pygmy chimpanzee, gorilla and human, one AP radiograph, one AP scout image[5] and one CT

[5]Although obtained and digitally reconstructed on a GE CT Scanner, in appearance a scout image is basically equivalent to a radiograph. The primary purpose of a scout image is not diagnostic, but rather to plan and display the location where CT slices are obtained.

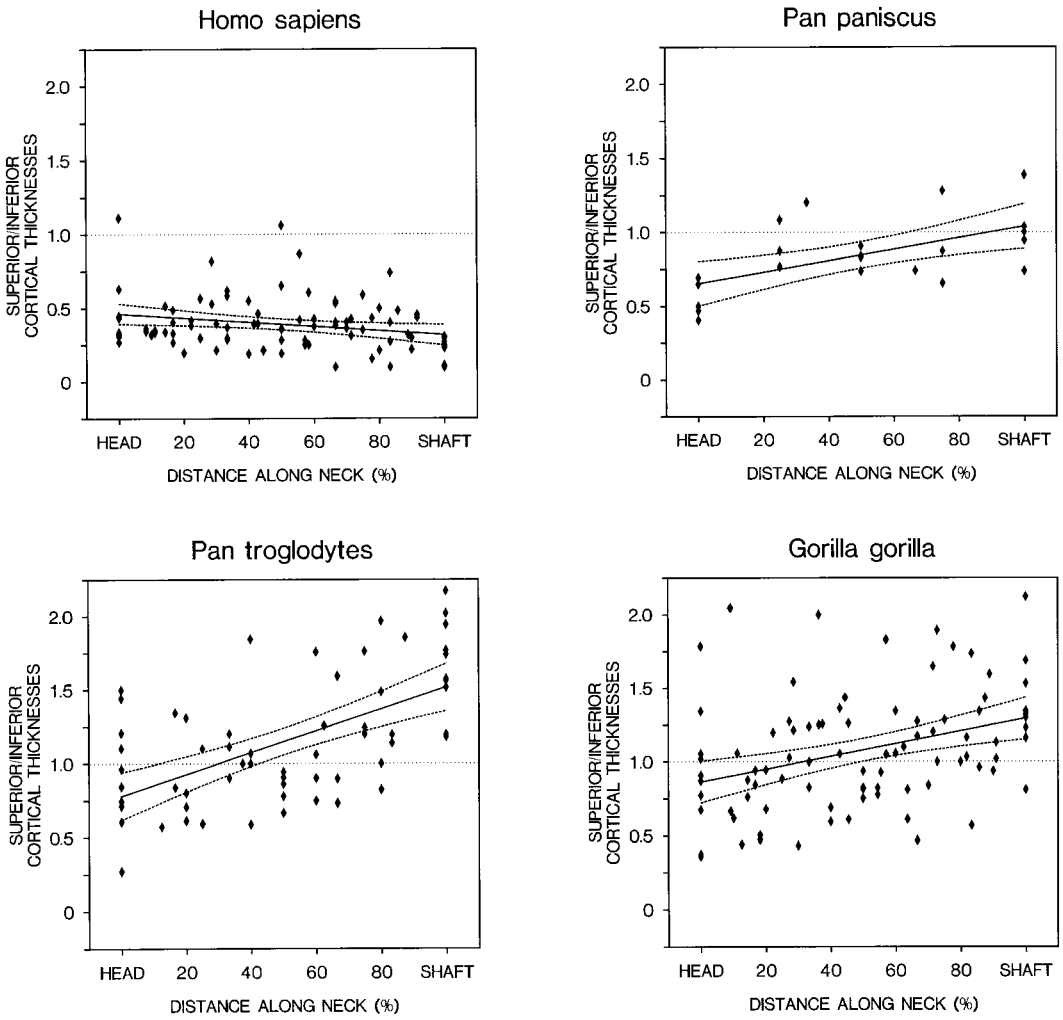

Fig. 6. Ratio of superior over inferior cortical thicknesses along the femoral neck in *Homo sapiens, Pan paniscus, Pan troglodytes,* and *Gorilla gorilla.* Least squares regression lines with 95% confidence intervals are provided *only to illustrate* typical relative cortical thicknesses along the femoral neck for each taxon, as we do not expect cortical thicknesses to vary linearly (sensu stricto) along the femoral neck.

image through the femoral neck (see below). For the siamang and common chimpanzee, only the above quotation was provided (Stern and Susman, 1991).

Second, their (Stern and Susman, 1991) inclusion of a single spider monkey is puzzling. The remainder of their (Stern and Susman, 1991) sample consisted entirely of hominoids, but Susman has recently voiced concern about comparisons of morphological non-equivalents (Susman, 1995). Even within hominoids, he (Susman, 1994) excluded gorillas from an analysis of hand morphology as it relates to toolmaking capabilities in early hominids because they "are morphologically distinct from early hominids" (Susman, 1995, p. 589).

Third, the radiograph of the human proximal femur presented by Stern and Susman (1991, Fig. 4) is also somewhat unusual (cf. Walker and Lovejoy, 1985). Curiously, instead of providing a simple original radiograph (Stern and Susman, 1991) obtained by similar methods to the others they pre-

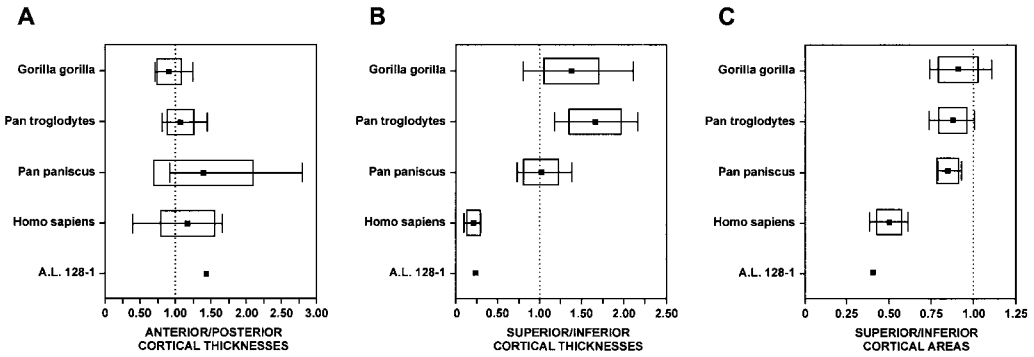

Fig. 7. At the neck-shaft junction, mean (■), standard deviation (□), and range (⊢⊣) in the ratios of **(A)** anterior over posterior cortical thickness; **(B)** superior over inferior cortical thickness; and **(C)** cortical area in the superior half over the inferior half.

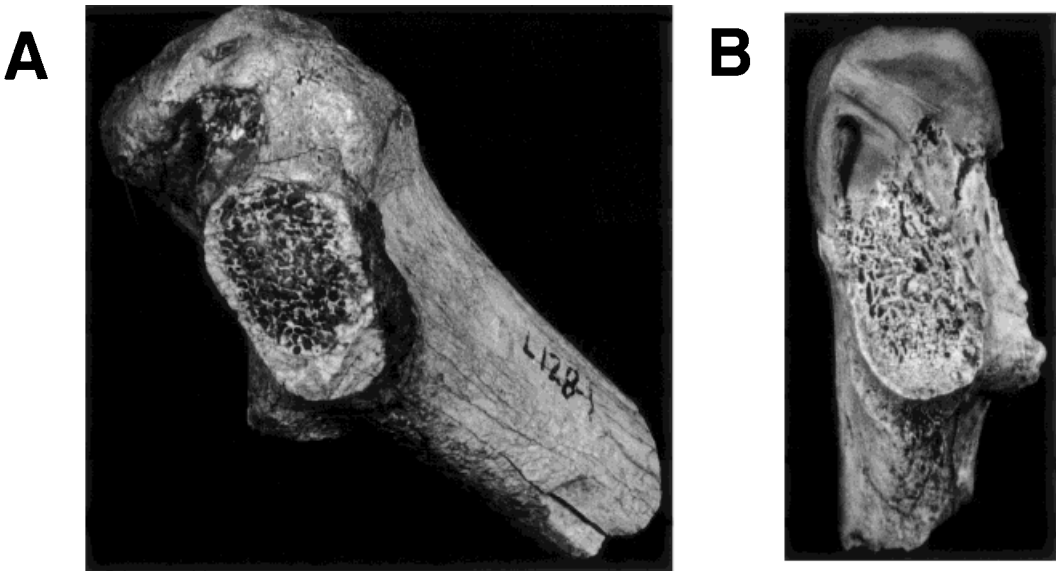

Fig. 8. Exposed section of the femoral neck at the neck-shaft junction in (**A**) A.L. 128-1 and **(B)** A.L. 211-1.

sented, their single human specimen was reproduced from a textbook figure (Wicke et al., 1987, Fig. 84).[6] While a respected source, this radiograph has been altered several times from its original form and may reflect the contrast increasing effects of the printing process. Indeed, before publication in the first German edition, "the original radiographs were electronically *contrast-enhanced* and converted into positives" (Wicke et al., 1987, p. VII, emphasis added), but later reproduced "as negatives" for the third German edition (Wicke et al., 1987, p. VI).[7] Clearly, a simple, direct radiograph of a human proximal femur would have been more comparable to those of the other pri-

[6]For example, Stern and Susman (1991) could have provided a radiograph of the specimen they used for their CT sample. However, even though Stern and Susman (1991) did not compare it to their other radiographs, the scout of this human proximal femur (Stern and Susman, 1991, Fig. 5) does show the more typical radiographic anatomy of the human proximal femur.

[7]The fourth English edition, from which Stern and Susman (1991) obtained the radiograph, was the translation of the third German edition.

mates presented (Stern and Susman, 1991, Fig. 4).

Therefore, only their (Stern and Susman, 1991, Fig. 5) single CT image of the pygmy chimpanzee can be used for comparison here. However, it was obtained nearer to the base of the head than to the neck-shaft junction (Stern and Susman, 1991, Fig. 5).[8] As a result, its location is not comparable to A.L. 129-1 and A.L. 211-1 (Fig. 8) or to more biomechanically relevant images of the neck-shaft junction (Fig. 7).[9] As Lovejoy (1988) stated:

> The neck acts as a cantilevered beam: a beam that is anchored at one end to a supporting structure (the shaft of the femur) and carries a load at the other end. Cantilevering results in high bending stresses at the beam's anchorage—compression along the bottom of the beam and tension along the top—and the stress increases along the length of the beam [p. 123].

Therefore, the anchorage of the femoral neck (i.e., the neck-shaft junction) is subjected to the highest bending stresses and is the most biomechanically relevant region to inspect for adaptations to locomotor habitus.

Given that cortical bone is weaker in tension than in compression (e.g., Currey, 1970), the bending stress distribution in a cantilevered beam (superior tension and inferior compression) dictates that cortical bone should be abundant in the superior femoral neck, absent other complicating factors such as the human abductor apparatus.[10] Indeed, this is true for the African apes, but not for the hominids (Figs. 4 through 8) even though their lower neck-shaft (collo-diaphyseal) angle and relatively longer femoral necks (Lovejoy et al., 1973) should produce much greater relative stresses at the neck-shaft junction (see also Lovejoy et al., in review). Clearly, there must be additional forces acting regularly on the hominid femoral neck.

Frankel (1960; see also Lovejoy, 1988) showed that, unlike the African apes, the abductors (*glutei medius* and *minimus*, anterior fibers of *gluteus maximus*, *tensor fascia femoris*, and *piriformis*) impart a compressive force on the femoral neck during stance phase. When this compression is added to the bending stresses due to cantilevering, tension along the superior aspect of the neck is largely negated and compression along the inferior aspect of the neck is increased. Therefore, at the neck-shaft junction in hominids (Figs. 4 through 8), thin superior cortical bone reflects minimal net stresses and thick inferior cortical bone reflects increased net stresses (Lovejoy, 1988).

Recently, Carter et al. (1989) related loading history to bone maintenance in the proximal femur by employing an iterative two-dimensional finite element model. They (Carter et al., 1989) modeled three different single-loading-directions, plus a more complex and realistic multiple-loading-directions case.[11]

Their (Carter et al., 1989) three single-loading-directions were chosen to represent the effects of the stance phase of gait (Fig. 9A) in combination with the extrema of motion (Figs. 9B and 9C), and their results "captured the major features of bony morphology" (Carter et al., 1989, p. 242). Their (Carter et al., 1989) second and third cases have important implications here.

Their (Carter et al., 1989) second case (Fig. 9B) mimics a cantilevered beam. The

[8]According to Stern and Susman's (1991, Fig. 5) scout image, they obtained three CT images through the neck: the first near the base of the head; the second, which they presented, close to the first but slightly more distal; and a third nearer the neck-shaft junction (which they did not illustrate).

[9]Stern and Susman's (1991) qualitative observation that "the inferior cortical bone was thicker" (p. 105) *can* occur in the proximal half of the femoral neck (Fig. 6). Importantly, however, such a simplification masks 1) the circumferentially thicker cortical bone throughout the femoral neck of African apes (Figs. 2 through 5; Stern and Susman, 1991, Fig. 5) and 2) dramatic cortical bone distribution differences between the African apes and hominids at the neck-shaft junction (Figs. 2 through 8).

[10]While bone responds to strain and not stress, we assume that a common stress distribution will produce a common strain distribution, and therefore a common shape response (i.e., cortical bone distribution in the proximal femoral neck), in African apes and hominids *if* the cortical bone of these taxa have the same material properties. We have no reason to doubt this assumption given that the bone tissue (i.e., material) properties for all terrestrial mammals are quite similar (e.g., see Selker and Carter, 1989, and discussion therein).

[11]For their different finite element analysis remodeling solutions, Carter et al. (1989) reported the distribution of bone morphology in terms of apparent density (ρ_a). Because apparent density is a volume average, $\rho_a = \frac{1}{V}\int_V \rho \, dV$ (where ρ is the true density of the hard tissue in the volume of interest, V), it incorporates the porosity of the volume (Fyhrie and Schaffler, 1995). Thus, the models reported by Carter et al. (1989) reflect the distribution of differential porosity in proximal femoral bone morphology. Although regions of relatively high apparent density could represent cancellous bone with *aligned*, relatively dense trabeculae, a fundamental difference between cortical bone and cancellous bone is their differential porosity (e.g., Schaffler and Burr, 1988). Moreover, both qualitative and quantitative observations of proximal femora (e.g., Figs. 2 through 8; Lovejoy et al., in review; Walker and Lovejoy, 1985) confirm the presence of a cortical shell of varying thickness surrounding cancellous bone. Therefore, while the boundary between cortical and cancellous bone cannot be precisely determined from the models generated by Carter et al. (1989), the relative thickness of regions of large apparent density along the superior and inferior margins of the femoral neck are almost certainly indicative of relative thickness of cortical bone along these margins.

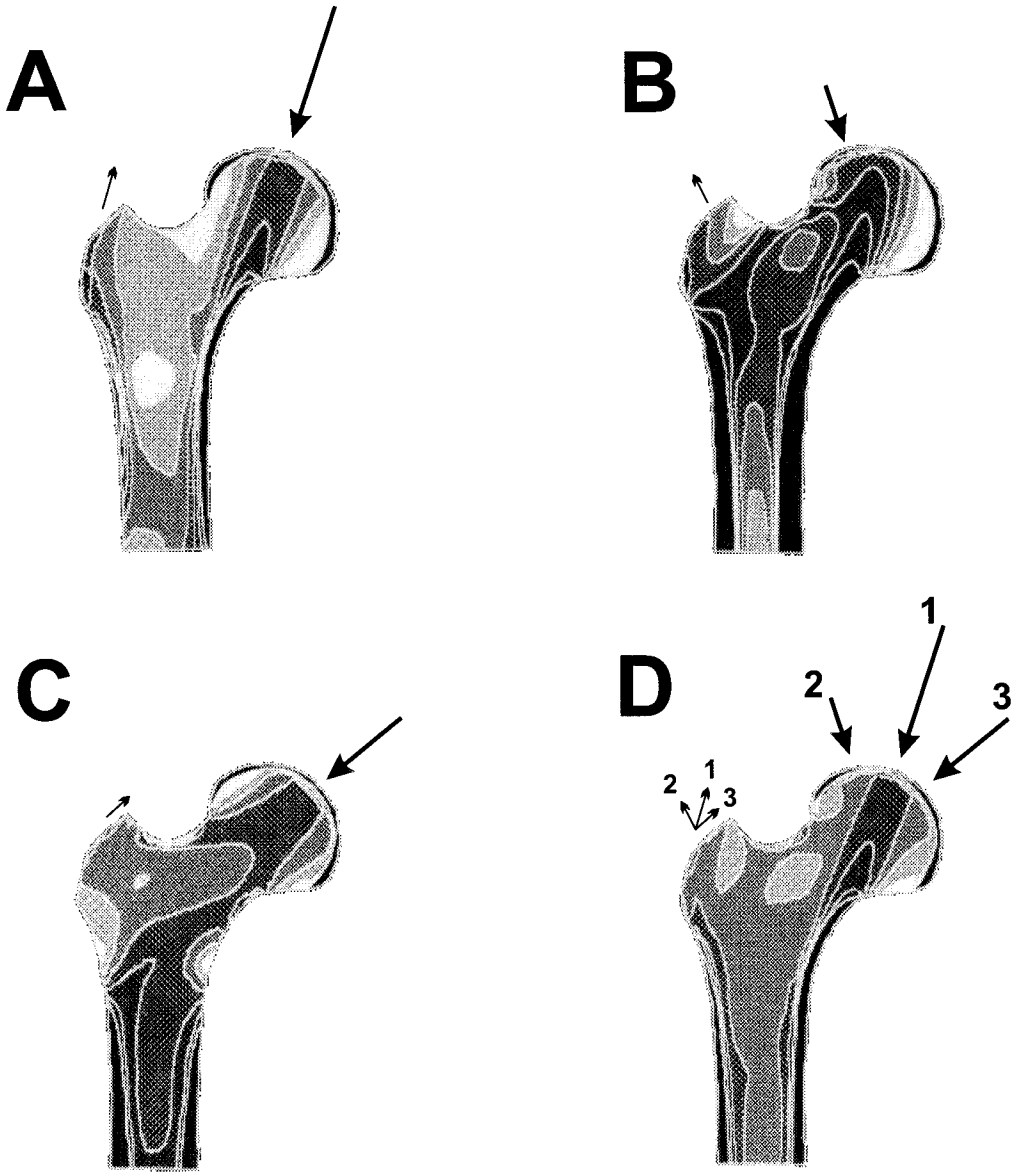

Fig. 9. Results obtained by Carter et al. (1989) for bone remodeling experiments using multiple two-dimensional finite element solutions. Apparent density increases from white to black. **(A)** Model based on single-loading-direction that represents the stance phase of gait (after Carter et al., 1989, Fig. 4, 3rd iteration). **(B)** Model based on single-loading-direction at extreme range of motion that mimics a cantilevered beam (after Carter et al., 1989, Fig. 5, 3rd iteration). **(C)** Model based on single-loading-direction at extreme range of motion that mimics pure compression (after Carter et al., 1989, Fig. 6, 3rd iteration). **(D)** Model based on multiple-loading-directions with predominant loading along the direction of the stance phase of gait and lesser loads at the extremes of range (after Carter et al., 1989, Fig. 10, 3rd iteration and M = 4.0). For details see Carter et al. (1989).

bending in the neck, with superior tension and inferior compression, produced increased apparent density along both the superior and inferior aspects of the neck (Carter et al., 1989). This model thus approximates the quadrupedal African apes in both loading (i.e., a hominid-like abductor apparatus is absent) and the resulting distribution of cortical bone.

Their (Carter et al., 1989) third case (Fig. 9C) demonstrated the effects of compression

in the neck. The result was decreased apparent density along the superior aspect of the neck, and increased apparent density along the inferior aspect of the neck (Carter et al., 1989). Therefore, while extreme, this model demonstrates the consequences of the muscular compressive forces present in hominids, but absent in the African apes.

Multiple-loading-directions (Fig. 9D), with predominant loading corresponding to that imposed during the stance phase of gait, and lesser loads being those produced at the extremes of the range of motion, produced a model with the "diaphyseal cortex and the orientation and density distributions of the [human] proximal femur" (Carter et al., 1989, p. 243). While an advance over the single-loading-direction cases, even this analysis is "a significant simplification of the actual loading history to which bones are exposed" (Carter et al., 1989, p. 242). Nonetheless, this model (Fig. 9D) bears a striking resemblance to the hominid proximal femur (Figs. 2 through 8; see also Lovejoy et al., in review; Walker and Lovejoy, 1985).

Carter and coworkers (1989) also concluded that "the greater the variation in loading conditions, the more subtle will be the variations in bone density since bone will be required in more diffuse areas" (p. 241). Therefore, relative to hominids, the circumferentially thicker cortical bone in the femoral neck of African apes reflects much greater *variation* in loading conditions (i.e., a less stereotypic loading pattern), and contrasts sharply with that of hominids.

The hominid condition must therefore be a response to the much more stereotypic loading pattern imposed by habitual bipedal locomotion with hip abduction to control pelvic tilt. That A.L. 129-1, A.L. 211-1 and MAK-VP-1/1 (see Lovejoy et al., in review) are indistinguishable from *H. sapiens* in their cortical distribution demonstrates the presence of an habitual human-like bipedality in the hominid lineage by the time of their appearance in the fossil record, and an absence of superior cortex in these same specimens further confirms the absence of a significant arboreal component to their locomotor repertoire.

Does this feature therefore qualify for Stern and Susman's (1991) definition of a "magic trait?" That is, does the hominid pattern of cortical distribution in the femoral neck *by itself* mean that *A. afarensis* (or for that matter *H. sapiens*) is incapable of arboreal behavior? Obviously, the answer is no. *By itself,* this feature only reflects a very stereotypic loading pattern imposed by habitual bipedality on the proximal femur. On the other hand, if the locomotor repertoire of *A. afarensis* had included a significant component of arboreality, their femoral necks should display circumferentially thicker cortical bone like those of the African apes. In other words, this feature does not tell us what *A. afarensis* was capable or incapable of *ever* doing (even modern humans occasionally climb trees); rather it is direct evidence of the locomotor *habitus* of this species.

Indeed, that is the very problem with Stern and Susman's (1991) concept of a "magic trait." The reason they (Stern and Susman, 1991) could not find a "magic trait" among Lovejoy's (1988) items of evidence was simply because "magic traits" do not exist. A single morphological trait can provide only one piece to a puzzle. Only after all individual pieces are assembled into a "total biomechanical pattern" (Lovejoy, 1975) can we begin to understand an animal's predominant behavioral habit. This is exactly what Lovejoy (1988) did in his review of the total biomechanical pattern manifested in the pelvis and proximal femur of hominids. As documented here, one of the paramount features in that pattern is the distribution of cortical bone in the femoral neck of hominids, a feature which demonstrates unequivocally that habitual terrestrial bipedality was the primary locomotor behavior of *A. afarensis.*

ACKNOWLEDGMENTS

We thank the Ethiopian Ministry of Culture and Sports Affairs, and the National Museum of Ethiopia for access to the fossil specimens. We thank the following for making the extant specimens available: Bryn Mader, American Museum of Natural History; Judy Chupasko, Terry McFadden, and Maria Rutzmoser at the Museum of Comparative Zoology; and David Begun, University of Toronto. We thank the following for making it possible to obtain and analyze the CT scans: Carol Burton and Anne MacDonald, Dana Farber Cancer Institute; Bruce Teeter, General Electric Medical Systems;

Biomedical Imaging Resource, Mayo Foundation; David Dean, then of New York University Medical Center; Nelly Patino, New York University Medical Center; CT Division, Picker International; and John Stears, University of Colorado Health Sciences Center. We also thank: Tim White for the photographs used in Figure 8; Bob Read for his assistance in the production of Figure 9; Lyman Jellema, Cleveland Museum of Natural History, for his assistance; and Gabriele Macho for her helpful comments.

LITERATURE CITED

Carter DR, Orr TE, and Fyhrie DP (1989) Relationships between loading history and femoral cancellous bone architecture. J. Biomech. *22:*231–244.

Christensen EE, Curry TS III, and Dowdey JE (1978) An Introduction to the Physics of Diagnostic Radiology. Philadelphia: Lea and Febiger.

Clark JD, Asfaw B, Assefa G, Harris JWK, Kurashina H, Walter RC, White TD, and Williams MAJ (1984) Palaeoanthropological discoveries in the Middle Awash Valley, Ethiopia. Nature *307:*423–428.

Currey JD (1970) The mechanical properties of bone. Clin. Orthop. *73:*210–231.

Frankel VH (1960) The Femoral Neck: Function, Fracture Mechanism, Internal Fixation; An Experimental Study. Springfield, IL: CC Thomas.

Fyhrie DP, and Schaffler MB (1995) The adaptation of bone apparent density to applied load. J. Biomech. *28:*135–146.

Hendee WR (1983) The Physical Principles of Computed Tomography. Boston: Little, Brown.

Johanson DC, White TD, and Coppens Y (1978) A new species of the genus *Australopithecus* (Primates: Hominidae) from the Pliocene of Eastern Africa. Kirtlandia *28:*1–14.

Johanson DC, Lovejoy CO, Kimbel WH, White TD, Ward SC, Bush ME, Latimer BM, and Coppens Y (1982a) Morphology of the Pliocene partial hominid skeleton (A.L. 288-1) from the Hadar Formation, Ethiopia. Am. J. Phys. Anthropol. *57:*403–451.

Johanson DC, Taieb M, and Coppens Y (1982b) Pliocene hominids from the Hadar Formation, Ethiopia (1973–1977): Stratigraphic, chronologic, and paleoenvirionmental contexts, with notes on homonid morphology and systematics. Am. J. Phys. Anthropol. *57:*373–402.

Koehler PR, Anderson RE, and Baxter B (1979) The effects of computed tomography viewer controls on anatomical measurements. Radiology *130:*189–194.

Lovejoy CO (1975) Biomechanical perspectives on the lower limb of early hominids. In RH Tuttle (ed.): Primate Functional Morphology and Evolution. The Hague: Mouton, pp. 291–326.

Lovejoy CO (1988) Evolution of human walking. Sci. Am. *259:*118–125.

Lovejoy CO, Heiple KG, and Burstein AH (1973) The gait of *Australopithecus.* Am. J. Phys. Anthropol. *38:*757–780.

Lovejoy CO, Johanson DC, and Coppens Y (1982) Hominid lower limb bones recovered from the Hadar Formation: 1977–1974. Am. J. Phys. Anthropol. *57:*679–700.

Lovejoy CO, White TD, Ohman JC, Meindl RS, Latimer B, Cohn MJ, Heiple KG, and Simpson SW (in review) The Maka femur: Its morphology and biomechanics and their bearing on the locomotor status of *Australopithecus afarensis* when viewed from the perspective of the morphologic code. Am. J. Phys. Anthropol.

Ohman JC (1993a) Computer software for estimating cross sectional geometric properties of long bones with concentric and elliptical models. J. Hum. Evol. *25:*217–227.

Ohman JC (1993b) Cross Sectional Geometric Properties from Biplanar Radiographs and Computed Tomography: Functional Application to the Humerus and Femur in Hominoids. Ph.D. dissertation, Kent State University.

Ohman JC (in review) An empirical comparison of torsional strength measures in hominoid humeri and femora. Am. J. Phys. Anthropol.

Ohman JC, and Krochta TJ (in press) Cross sectional geometric properties of long bones: Automatic estimation directly from computed tomography image data. Comput. Biomed. Res.

Ohman JC, Mensforth RP, and Latimer B (1997) Age-related osteopenia in *Gorilla gorilla* and *Pan troglodytes.* Am. J. Phys. Anthropol. Suppl. *24:*181 (abstract).

Reed KE, Kitching JW, Grine FE, Jungers WL, and Sokoloff L (1993) Proximal femur of *Australopithecus africanus* from Member 4, Makapansgat, South Africa. American J. Phys. Anthropol. *92:*1–15.

Schaffler MB, and Burr DB (1988) Stiffness of compact bone: Effects of porosity and density. J. Biomech. *21:*13–16.

Selker F, and Carter DR (1989) Scaling of long bone fracture strength with animal mass. J. Biomech. *22:*1175–1183.

Spoor CF, Zonneveld FW, and Macho GA (1993) Linear measurements of cortical bone and dental enamel by computed tomography: Applications and problems. Am. J. Phys. Anthropol. *91:*469–484.

Spoor F, Wood B, and Zonnenveld F (1994) Implications of early hominid labyrinthine morphology for evolution of human bipedal locomotion. Nature *269:*645–648.

Sprawls P Jr (1987) Physical Principles of Medical Imaging. Rockville: Aspen.

Stern JT Jr, and Susman RL (1991) "Total morphological pattern" versus the "magic trait:" Conflicting approaches to the study of early hominid bipedalism. In Y Coppens and B Senut (eds.); Origine(s) de la Bipédie chez les Hominidés. Paris: Editions du Centre National de la Recherche Scientifique, pp. 99–111.

Sumner DR, Morbeck ME, and Lobick JJ (1989) Apparent age-related loss among adult female Gombe chimpanzees. Am. J. Phys. Anthropol. *79:*225–234.

Susman RL (1994) Fossil evidence for early hominid tool use. Science *265:*1570–1573.

Susman RL (1995) Thumbs, tools, and early humans. Science *268:*586–589.

Walker RA, and Lovejoy CO (1985) Radiographic changes in the clavicle and proximal femur and their use in the determination of skeletal age at death. Am. J. Phys. Anthropol. *68:*67–78.

White TD (1984) Pliocene hominids from the Middle Awash, Ethiopia. Courier Forschungintitut Senckenberg *69:*57–68.

Wicke L, Firbas W, Schmiedl R, and Taylor AN (1987) Atlas of Radiologic Anatomy. Baltimore: Urban and Schwarzenberg.

Zatz LM (1981) Basic principles of computed tomography scanning. In TH Newton and DG Potts (eds.): Radiology of the Skull and Brain: Technical Aspects of Computed Tomography. Vol. 5. St. Louis: C.V. Mosby, pp. 3853–3876.